

A novel microbead-based microfluidic device for rapid bacterial identification and antibiotic susceptibility testing

J. He · X. Mu · Z. Guo · H. Hao · C. Zhang · Z. Zhao ·
Q. Wang

Received: 24 March 2014 / Accepted: 3 June 2014 / Published online: 5 July 2014
© Springer-Verlag Berlin Heidelberg 2014

Abstract Effective treatment of infectious diseases depends on the ability to rapidly identify the infecting bacteria and the use of sensitive antibiotics. The currently used identification assays usually take more than 72 h to perform and have a low sensitivity. Herein, we present a microbead-based microfluidic platform that is highly sensitive and rapid for bacterial detection and antibiotic sensitivity testing. The platform includes four units, one of which is used for bacterial identification and the other three are used for susceptibility testing. Our results showed that *Escherichia coli* O157 at a cell density range of 10^1 – 10^5 CFU/ μ L could be detected within 30 min. Additionally, the effects of three antibiotics on *E. coli* O157 were evaluated within 4–8 h. Overall, this integrated microbead-based microdevice provides a sensitive, rapid, reliable, and highly effective platform for the identification of bacteria, as well as antibiotic sensitivity testing.

Introduction

Infectious diseases are a leading cause of death [1, 2]. Over 95 % of these deaths are caused by the lack of proper diagnosis and treatment [3]. Conventional methods of diagnosis are time-consuming and cumbersome. In addition, these methods are not feasible for synchronous or high-throughput screening. Therefore, it is critical to develop a tool for shortening the time necessary to identify infectious pathogens and an effective antibiotic regimen for treatment.

Microfluidics is an attractive platform for rapid and multiple analysis [4–12]. Immunomicrobeads coated with a specific antibody for the target pathogen provide a simple and direct method to capture and enrich the target pathogen. This capture/enrichment method (referred to as immunocapture) increases the effective concentration of the bacterium and allows target bacteria to accumulate on the surface of microbeads. This technique has been commonly used for pathogenic separation and detection in microfluidic devices [6, 7]. Similar techniques, such as magnetic immunomicrobeads, have also been used for rapid functional analysis and susceptibility screening [8, 9]. However, these methods lack the capacity for high-throughput screening and the implementation of multiplexed biological assays. Here, we introduce an immunomicrobead-based microfluidic device that can be used for both rapid bacterial identification and antibiotic sensitivity testing. This technology offers at least two advantages: (1) two assays (bacterial identification and drug sensitivity testing) can be performed with a single microfluidic platform and (2) each assay can be performed using a low-density bacterial sample. This technology will reduce the time needed and increase the efficiency to diagnose bacterial infections, eventually enabling patient-specific antibiotic regimens.

J. He and X. Mu contributed equally to the article.

J. He · Z. Guo · H. Hao · Q. Wang (✉)
Department of Respiratory Medicine, The Second Hospital,
Dalian Medical University, Dalian 116023, China
e-mail: wqdlmu@163.com

J. He
e-mail: jiarui.he618@gmail.com

X. Mu
Department of Respiratory and Critical Care Medicine,
Peking University People's Hospital, Beijing 100044, China
e-mail: xinlin169@163.com

C. Zhang
Department of Endocrinology Medicine, The Second Hospital,
Dalian Medical University, Dalian 116023, China

Z. Zhao (✉)
Department of Breast Surgery Medicine, The Second Hospital,
Dalian Medical University, Dalian 116023, China
e-mail: dlzhaowz@163.com

Materials and methods

Microfluidic chip fabrication

The schematic representation of the microfluidic chip is shown in Fig. 1A. The microfluidic chip consists of four units sharing a common outlet. One unit was utilized for the identification of bacteria in a sample (unit *a*) and the other three units (units *b*, *c*, and *d*) were used to test the susceptibility of bacteria to three different antibiotics in parallel. Figure 1B shows the details of unit *a*, which includes a sample inlet (1.5-mm diameter) and a capture chamber. The capture chamber (2 mm×4 mm×100 μm) is enclosed by many cuboid micropillars (black dotted line). The distance between neighboring micropillars is 60 μm and it was designed to hold a single layer of glass microbeads (average diameter=70 μm; Mianyang Guangyao New Material Co., Mianyang, Sichuan, China). Figure 1C shows the details of unit *b*, which consists of a linear concentration gradient generator (CGG), five downstream parallel mixture chambers, and the corresponding monitoring chamber. The unit has two inlets (1.5-mm diameter), used for medium, drug, or bacterial solution perfusion, and the corresponding cascade microchannels (10 mm×200 μm×100 μm). The CGG utilized diffusive mixing to generate a mixture of the two inlets at the cascade microchannels and could generate gradient concentrations of 0:1:2:3:4 theoretically based on the formula in a previous research [11]. Unit *b* also has two clips (clip 1 and clip 2) that serve as valves to control the liquid stream in the upper and lower microchannels. The workflow of units *a* and *b/c/d* is illustrated in Figs. 1D, E. With the entire device, bacteria could be identified, and then the susceptibility of bacteria to three antibiotics could be tested.

The microfluidic device was fabricated with polydimethylsiloxane (PDMS, Sylgard 184, Dow Corning, Midland, MI, USA), and the assembly was placed on a glass slide to create an irreversible seal. The microfluidic device was sterilized overnight with UV light. Nonspecific interactions between the chip surface and cells or antibiotics were minimized by coating the walls of the fluid layer and the glass coverslip with 1 % bovine serum albumin.

Validation of the microfluidic chip

To validate the feasibility of the microfluidic platform for biological studies, *Escherichia coli* O157 at the same initial concentration was cultured in 96-well plates and in the microfluidic chip. The growth states of the bacterial cells were monitored by recording the optical density at a wavelength of 600 nm every 2 h during a period of 16 h. In addition, rhodamine 123 (Rh-123, Sigma Aldrich, St. Louis, MO, USA) was used to validate the performance of the CGG. Culture medium with or without 50 mM Rh-123 was introduced into a chip unit (units *b*, *c*, or *d*) from the drug and

Fig. 1 Schematic of the integrated microfluidic device for bacterial identification and antibiotic sensitivity testing. **A** Diagram (*left*) and a picture (*right*) of the microfluidic device. **B** Enlarged diagram of unit *a*. **C** Enlarged diagram of unit *b*. **D** Workflow of unit *a*. ① Bacteria were injected into the unit. ② The bacteria mixed with the antibody (AB)-coated microbeads to form microbeads–bacteria complexes. ③ A mixture of monoclonal rabbit anti-*Escherichia coli* antibody (1:100 dilution, Abcam) and FITC-conjugated goat anti-rabbit polyclonal antibody (1:200 dilution, Santa Cruz Biotechnology) was injected into the unit, and the fluorescence intensity was measured using a fluorescence microscope. **E** Workflow of units *b*, *c*, or *d*. ① Bacteria were injected into the mixture chamber. ② Antibiotics [norfloxacin (12.8 μg/mL), ceftriaxone (8 μg/mL), or ampicillin (80 μg/mL)] were then injected into the microchannels to generate a series of gradient concentrations of the antibiotic. ③ SYBR green I, a fluorescence dye that only stains live cells, was added to the mixture chambers. ④ The mixture of the bacteria, antibiotic, and SYBR green dye was allowed to mix with AB-coated microbeads to form microbeads–bacteria complexes. ⑤ The fluorescence of SYBR green was captured by a fluorescence microscope and the fluorescence intensity was measured

medium inlets; a series of solutions containing different concentrations of Rh-123 were formed in the winding microchannels before entering the corresponding downstream mixture chambers. The junctions between the CGG and the mixture chambers were imaged with an inverted fluorescence microscope (Leica, DMI4000), and the fluorescence intensities of the Rh-123 were quantified and compared with the theoretical data.

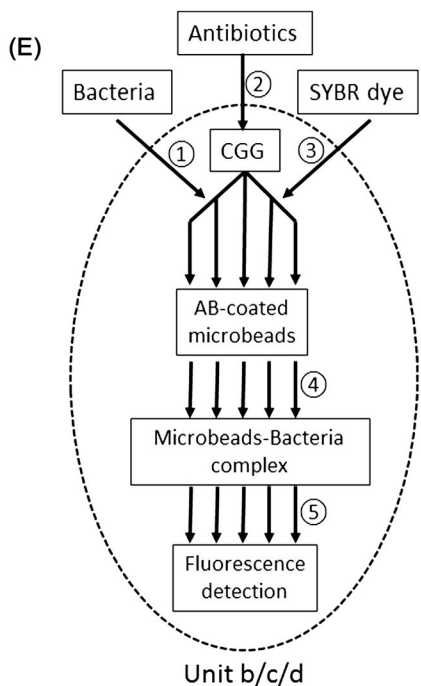
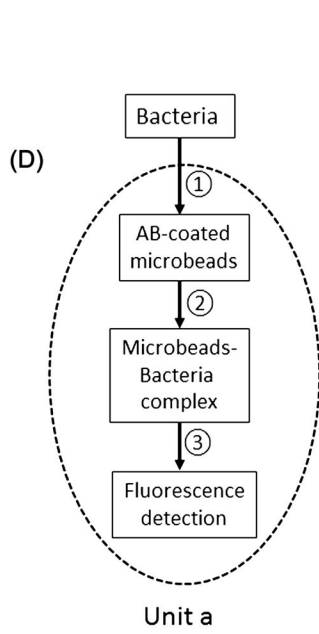
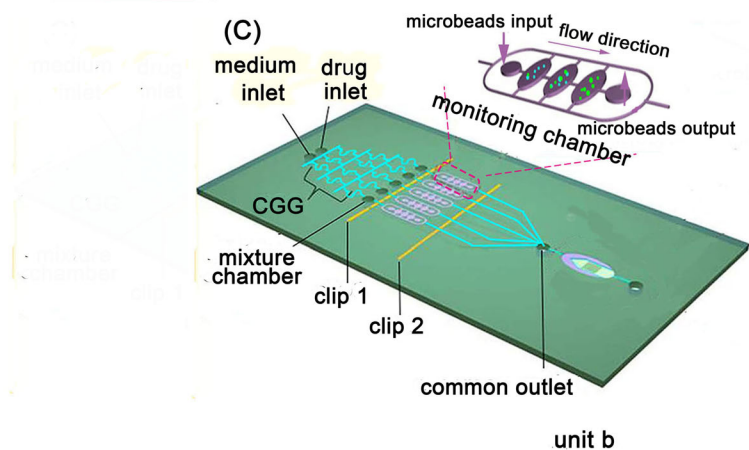
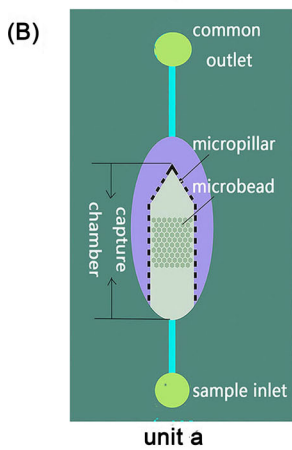
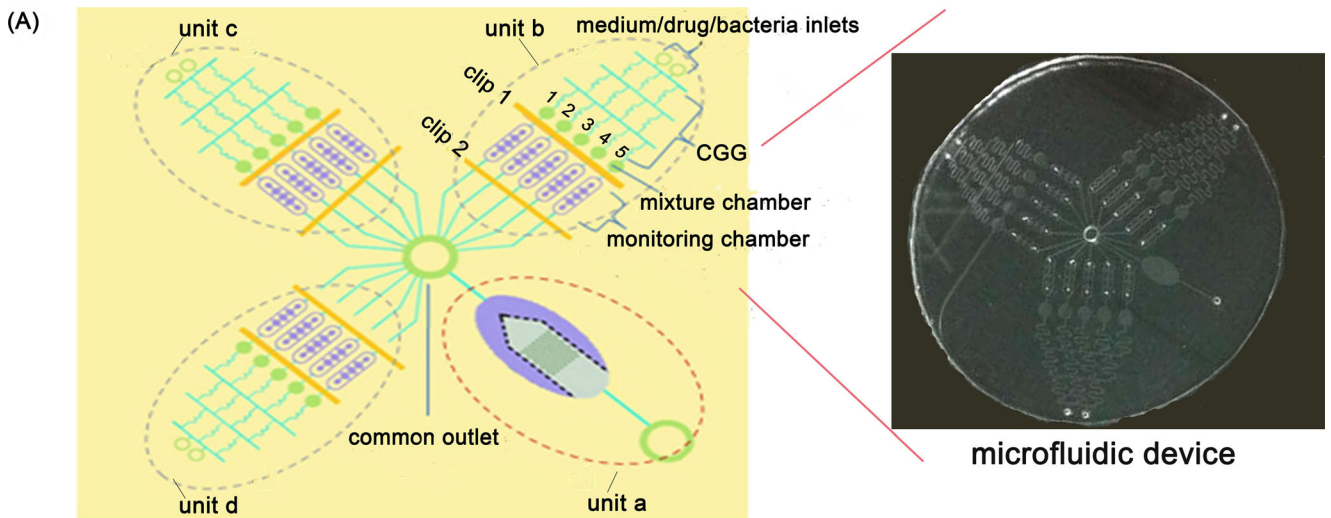
Bacterial cell culture

E. coli O157 (ATCC 35150, ATCC, Rockville, MD, USA) was used as the target bacteria. *E. coli* (ATCC 25922) and *Staphylococcus aureus* (ATCC6538) were used as control strains to evaluate the specificity for pathogenic identification. Bacterial strains were routinely cultivated in brain heart infusion (BHI) broth (Remel, Lenexa, KS, USA), and bacterial concentrations were determined by the standard plating count method (PCM).

Identification of *E. coli* O157 on the microfluidic chip

Immobilization of antibodies on microbeads was conducted as described previously [13]. To identify whether the microbeads have the ability to capture *E. coli* O157, 1 μL (10⁵ CFU) of bacterial solution was incubated with the coated microbeads in the capture chamber for 5 min to form a bacteria–microbead complex through immunoreactions. The microbeads were observed by a scanning electron microscope (SEM) (Quanta™ 650 FEG, USA).

The capture efficiency of chip unit *a* for different concentrations of *E. coli* O157 was tested using the PCM. Briefly, the glass microbeads were divided into experimental groups (coated with antibody) and control groups (not coated). First, 5 mg of the glass microbeads suspended in 100 μL of phosphate-buffered saline were injected into the chamber via a syringe



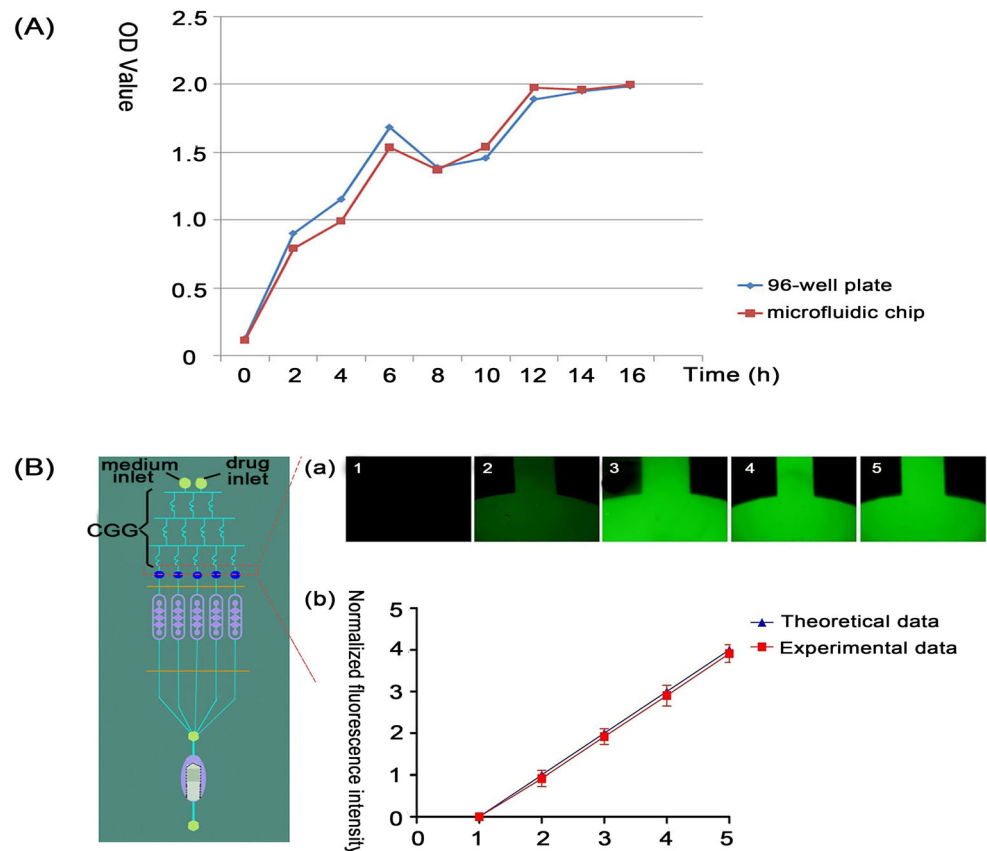
pump (Baoding Longer Precision Pump Co., Ltd., China) to form a microbead monolayer in the capture chamber. Next, 1 μL of an *E. coli* O157 suspension with concentrations ranging from 10^1 CFU/ μL to 10^6 CFU/ μL was injected into the unit slowly. The capture efficiency of the microbeads was calculated according to the following formula:

$$\text{Capture rate of chip unit}(\%) = \frac{(\text{Initial cell concentration} - \text{Cell concentration at outlet})}{\text{Initial cell concentration}} \times 100\% (\text{cell concentration was measured by the PCM})$$

Image processing and analysis

Images were taken using an inverted fluorescence microscope (Leica, DMI4000) with a 10×0.3 NA objective equipped with a CCD camera (Retiga 2000R, QImaging). FITC or SYBR green was imaged at an excitation wavelength of 490–495 nm and an emission wavelength of 525–530 nm. Fluorescence intensity was measured using Image-Pro[®] Plus 6.0 software (Media Cybernetics, Silver Spring, MD, USA). The fluorescence signal from the unoccupied immunomicrobeads was considered as background and subtracted from the signal.

Fig. 2 Validation of the microfluidic chip. **A** The growth curves of *Escherichia coli* O157 cultured in the microfluidic chip and a 96-well plate over a period of 16 h. **B** Performance validation of the concentration gradient generator (CGG) in the microfluidic device. **a** Fluorescence intensities of rhodamine 123 (Rh-123) in the mixing channels connecting the CGG and the mixture chambers [1–5 represent mixing channel 1 (close to the medium inlet) to channel 5 (close to the drug inlet), respectively]. **b** Quantified comparison of the actual and theoretical data for the fluorescence intensity of different concentrations of Rh-123 solution generated by the CGG



Statistical analyses

To evaluate the reliability of the experimental results, each experiment was repeated at least three times. Data were presented as means \pm standard deviation. A paired Student's *t*-test was used to compare the study groups. Significance was defined at $p \leq 0.05$. All statistical analyses were performed using SPSS 12.0 software (SPSS Inc.).

Results

Validation of the microfluidic chip

To validate the feasibility of the microfluidic platform for biological studies, we monitored the growth of *E. coli* O157 cultured in the microfluidic chip and compared it with that grown in 96-well plates. As shown in Fig. 2A, the growth curve for *E. coli* O157 cells in the chip was in close agreement with that in the 96-well plate for a period of 16 h. The statistical analysis showed that there were no significant differences between the two curves ($p > 0.05$).

To validate the CGG in the microfluidic device, the experimental gradient values were compared with the theoretical values, using Rh-123 as an indicator. There was good agreement between the experimental and theoretical data (correlation coefficient=0.9953) (Fig. 2B), indicating the feasibility of the CGG.

Identification of *E. coli* O157 on the microfluidic device

An SEM was used to examine whether the antibody-coated microbeads have the capability of capturing bacteria. As shown in Fig. 3, a large amount of *E. coli* O157 was present on the surface of a microbead selected randomly, indicating that the microbeads had a high capacity for specific capture.

The capture efficiencies of *E. coli* O157 cells in the experimental groups and the control groups were examined. As shown in Fig. 4, for the experimental groups, the capture rate was 85–92 %, with the bacterial concentrations varying from 4×10^1 CFU/ μ L to 4×10^5 CFU/ μ L. The capture rate was only 61.41 % when the bacterial concentration reached 4×10^6 CFU/ μ L. This finding was probably because the amount of bacteria in the sample was much larger than the number of antibody sites on the glass microbeads. For the control groups, the capture rates were all below 20 %, which was ascribed to nonspecific adsorptions. These results suggest that the antibody-coated microbeads provide ideal capture efficiency when the bacterial sample concentrations range from 4×10^1 CFU/ μ L to 4×10^5 CFU/ μ L.

We further validated the capture efficiency and specificity by fluorescence imaging of the FITC-labeled secondary antibody. Images were taken, and the fluorescence intensity of the bacteria at various concentrations was measured. As shown in Fig. 5A, the bacterial concentration was directly proportional to the fluorescence intensity. Furthermore, as shown in Fig. 5B, there

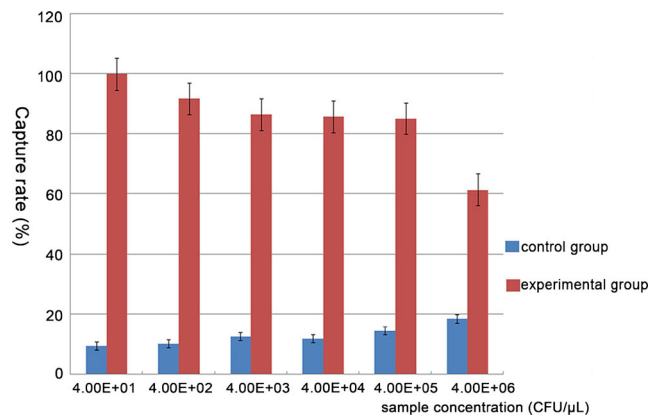


Fig. 4 The capture rates of the coated microbeads for various samples at different concentrations. The results were expressed as mean \pm standard deviation. The differences between the experimental groups and their corresponding control groups were statistically significant ($p < 0.05$)

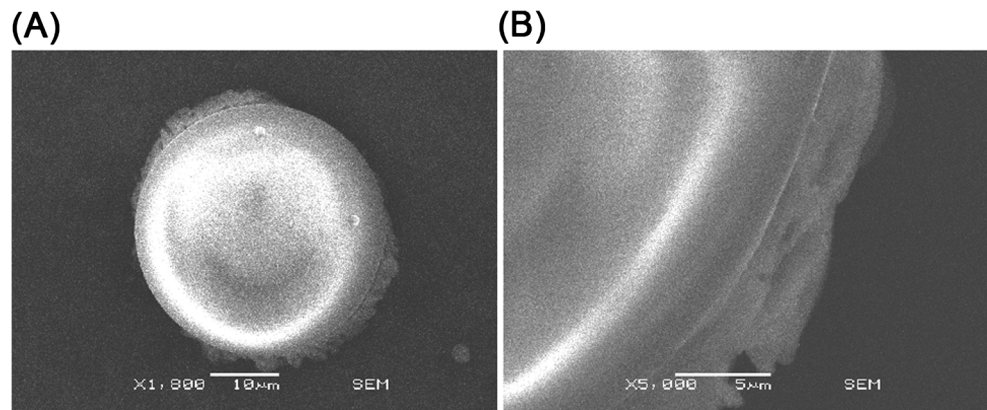
was a correlation between the bacterial concentration and the immunofluorescence measurement. These data demonstrate that our platform can be used for the quantitative determination of bacterial concentrations ranging from 10^1 to 10^5 CFU/ μ L, with high sensitivity.

The bacterial specificity was also assayed. As controls, *E. coli* (ATCC 25922) and *S. aureus* (ATCC 6538) diluted to the same concentration as *E. coli* O157 (10^5 CFU/ μ L) were tested. As shown in Fig. 5C, bright fluorescence was observed with *E. coli* O157, but almost no fluorescence was seen from the two control strains, indicating that our platform could specifically recognize *E. coli* O157.

Antibiotic susceptibility of *E. coli* O157

We employed chip units *b*, *c*, and *d* to test the susceptibility of *E. coli* O157 to norfloxacin, ceftriaxone, and ampicillin. For norfloxacin, the gradient concentrations were 0 (control group), 1.6, 3.2, 4.8, and 6.4 μ g/mL; for ceftriaxone, they were 0 (control group), 1, 2, 3, and 4 μ g/mL; and for

Fig. 3 Scanning electron microscope (SEM) pictures of *E. coli* O157 attached to a random anti-*E. coli*O157 antibody-modified microbead: **A** magnification, $\times 1,800$; **B** magnification, $\times 5,000$



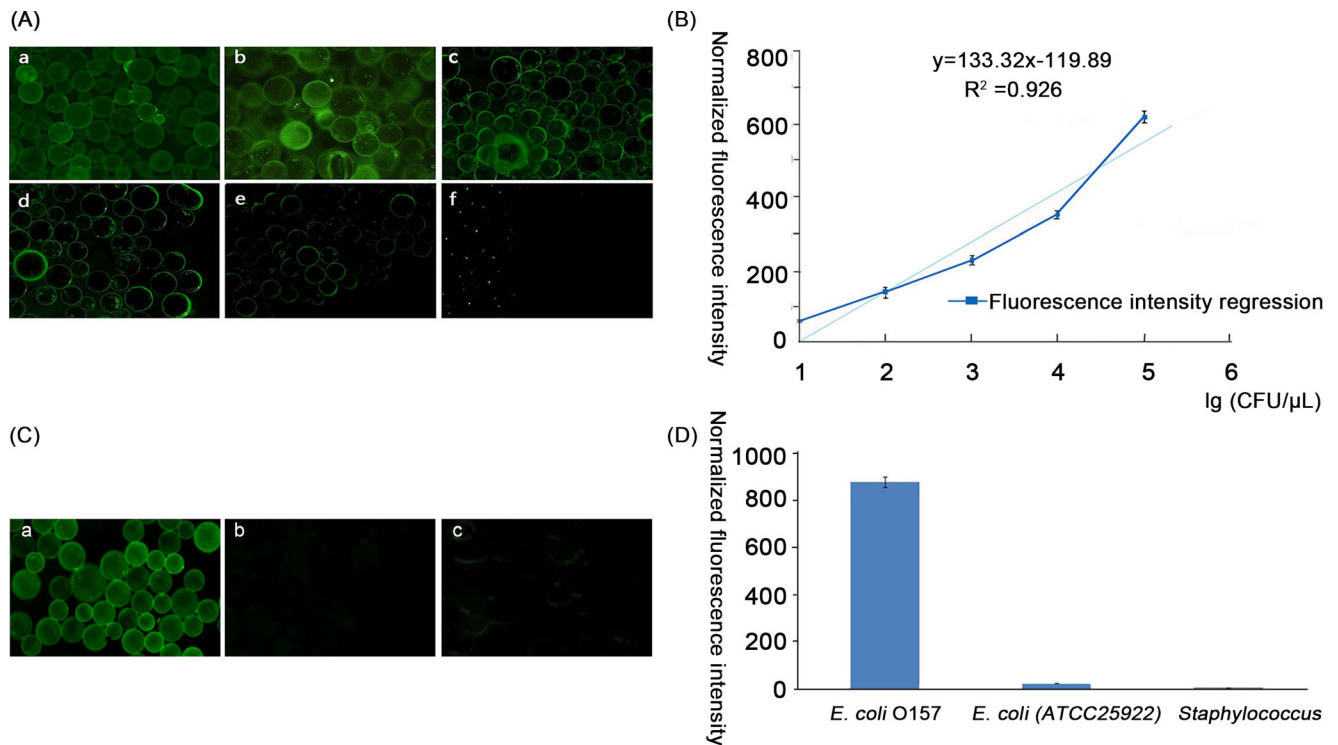


Fig. 5 Capture efficiency and specificity of the microfluidic device. **A** Fluorescence images of the capture chamber with different concentrations of *E. coli* O157 suspensions. **a–e** The representative concentrations of *E. coli* O157 samples were 4×10^5 CFU/ μ L, 4×10^4 CFU/ μ L, 4×10^3 CFU/ μ L, 4×10^2 CFU/ μ L, and 4×10^1 CFU/ μ L, respectively. **f**

Control group: sample with no bacteria. **B** Correlation between lg(CFU/ μ L) and fluorescence mean values obtained from antibody-modified microbeads in the capture chamber (with respect to the control group). **C** Fluorescence images of three strains. **a** *E. coli* O157, **b** *E. coli* (ATCC 25922), and **c** *S. aureus*. **D** Quantitative measurement of C

ampicillin, they were 0 (control group), 10, 20, 30, and 40 μ g/mL. With the increasing concentration of each antibiotic, an apparent change in the fluorescence signal was observed within 4–8 h (Fig. 6). These results indicated that both norfloxacin and ceftriaxone inhibited bacterial growth effectively, in a statistically significant dose- and time-dependent manner, whereas *E. coli* O157 was resistant to ampicillin when the concentration was less than 30 μ g/mL (Fig. 6).

The three antibiotic sensitivity tests were also determined by an absorbance-based assay performed in 96-well plates. The results were consistent with those obtained on the microfluidic platform. However, the 96-well plate assay takes a much longer time and consumes larger amounts of reagents (data not shown).

Discussion

In this study, we present a rapid and effective microbead-based microfluidic platform that could be used for both bacterial identification and antibiotic

sensitivity testing. Using this system, *E. coli* O157 could be distinguished from 1 μ L of sample with a concentration of 10^1 – 10^5 CFU/ μ L within 30 min. The antibiotic susceptibility to three antibiotics could be tested within 4–8 h. Unlike many microfluidic devices used currently [7, 14–16], another advantage of our system is the integration of four chip units into a multifunctional platform to enable multiple assays. As a result, the whole process from bacterial identification to relational antibiotic susceptibility testing could be carried out on a single platform, which greatly improves the application efficiency.

Sensitivity is a major concern in evaluating a microfluidic platform. Compared with previous detection platforms, we made some improvements to increase the sensitivity. First, the use of microbeads increases the surface area for antibody immobilization. Thus, the immunocapture efficiency was higher (85–92 %) than offline immunomagnetic separation, whose capture rates are 44–86 %, or the planar methods, whose capture rates are 21 % [17, 18]. Second, we modified the depth of the capture chamber, making it larger (100 μ m) than the diameter of the beads (70 μ m), so the beads could

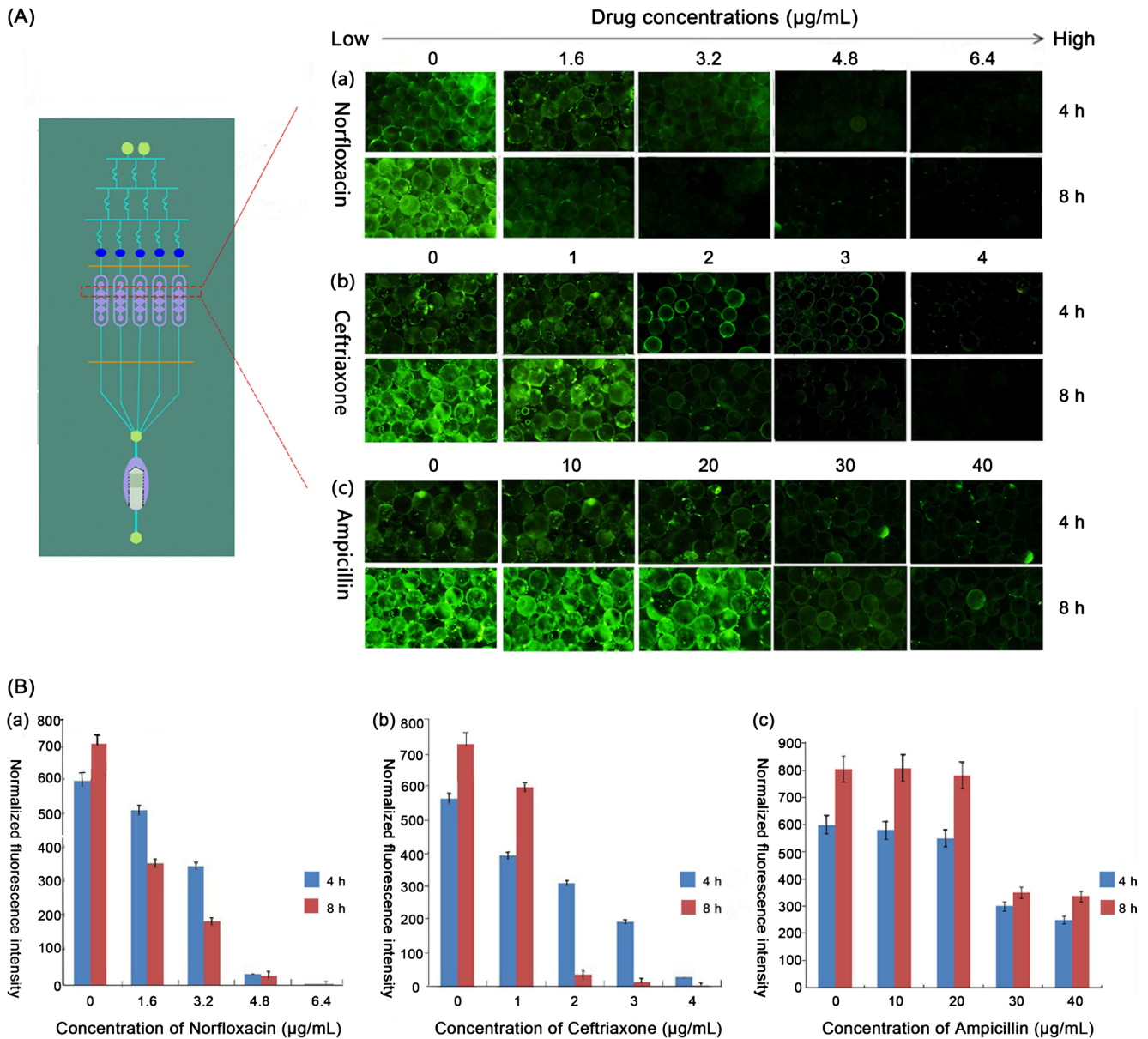


Fig. 6 Antibiotic sensitivity testing. **A** The fluorescence images of the corresponding monitoring chambers observed at 4 and 8 h after: **a** norfloxacin, **b** ceftriaxone, and **c** ampicillin treatment. **B** Temporal changes to the fluorescence intensity of the corresponding monitoring chambers

with gradient concentrations of norfloxacin (**a**), ceftriaxone (**b**), and ampicillin (**c**) at 4 and 8 h. The error bars represent standard deviations ($n=3$)

be aligned as a monolayer in the capture chamber. This design maximized the optical accessibility of bacteria to the detection light, and high fluorescence signal strength was achieved. Third, the use of CGG provided the advantage of automatically generating gradient concentrations of antibiotics. It greatly enhanced the efficiency of the antibiotic susceptibility tests and, therefore, enhanced the clinical applicability of this platform.

In summary, we demonstrated a microbead-based platform for rapid bacterial identification and antibiotic susceptibility testing. The presented immunocapture technology marks an

essential step towards this versatile platform for the integration of microbead- and cell-based assays. With this platform, the assay time was shortened from a typical 72 h to 8.5 h for the whole process. This integrated and flexible microfluidic platform has the potential to be incorporated as a routine clinical test device used for the early diagnosis and treatment of infectious diseases.

Acknowledgments This study was supported by the Special Fund for Health Scientific Research in the Public Interest from the National Health and Family Planning Commission of China (no. 201202011).

Conflict of interest The authors declare no conflict of interest.

References

1. Boedicker JQ, Li L, Kline TR, Ismagilov RF (2008) Detecting bacteria and determining their susceptibility to antibiotics by stochastic confinement in nanoliter droplets using plug-based microfluidics. *Lab Chip* 8:1265–1272. doi:10.1039/b804911d
2. Carrigan SD, Scott G, Tabrizian M (2004) Toward resolving the challenges of sepsis diagnosis. *Clin Chem* 50:1301–1314. doi:10.1373/clinchem.2004.032144
3. Nguyen HB, Rivers EP, Abrahamian FM, Moran GJ, Abraham E, Trzeciak S, Huang DT, Osborn T, Stevens D, Talan DA (2006) Severe sepsis and septic shock: review of the literature and emergency department management guidelines. *Ann Emerg Med* 48:28–54. doi:10.1016/j.annemergmed.2006.02.015
4. Sauer-Budge AF, Mirer P, Chatterjee A, Klapperich CM, Chargin D, Sharon A (2009) Low cost and manufacturable complete microTAS for detecting bacteria. *Lab Chip* 9:2803–2810. doi:10.1039/B904854E
5. Yager P, Edwards T, Fu E, Helton K, Nelson K, Tam MR, Weigl BH (2006) Microfluidic diagnostic technologies for global public health. *Nature* 442:412–418. doi:10.1038/nature05064
6. Mujika M, Arana S, Castaño E, Tijero M, Vilares R, Ruano-López JM, Cruz A, Sainz L, Berganza J (2009) Magneto-resistive immunosensor for the detection of *Escherichia coli* O157:H7 including a microfluidic network. *Biosens Bioelectron* 24:1253–1258. doi:10.1016/j.bios.2008.07.024
7. Srinivasan B, Varshney M, Tung S, Li Y (2005) A microfluidic filter chip for highly sensitive chemiluminescence detection of *E. coli* O157:H7. In: Proceedings of the ASME 2005 International Mechanical Engineering Congress and Exposition, Orlando, Florida, USA, November 2005. doi:10.1115/IMECE2005-81881
8. Kinnunen P, Sinn I, McNaughton BH, Newton DW, Burns MA, Kopelman R (2011) Monitoring the growth and drug susceptibility of individual bacteria using asynchronous magnetic bead rotation sensors. *Biosens Bioelectron* 26:2751–2755. doi:10.1016/j.bios.2010.10.010
9. Sinn I, Kinnunen P, Albertson T, McNaughton BH, Newton DW, Burns MA, Kopelman R (2011) Asynchronous magnetic bead rotation (AMBR) biosensor in microfluidic droplets for rapid bacterial growth and susceptibility measurements. *Lab Chip* 11:2604–2611. doi:10.1039/C0LC00734J
10. Sia SK, Whitesides GM (2003) Microfluidic devices fabricated in poly(dimethylsiloxane) for biological studies. *Electrophoresis* 24:3563–3576. doi:10.1002/elps.200305584
11. Jeon NL, Dertinger SK, Chiu DT, Choi IS, Stroock AD, Whitesides GM (2000) Generation of solution and surface gradients using microfluidic systems. *Langmuir* 16:8311–8316. doi:10.1021/la000600b
12. Duffy DC, McDonald JC, Schueller OJ, Whitesides GM (1998) Rapid prototyping of microfluidic systems in poly(dimethylsiloxane). *Anal Chem* 70:4974–4984. doi:10.1021/ac980656z
13. Guan X, Zhang HJ, Bi YN, Zhang L, Hao DL (2010) Rapid detection of pathogens using antibody-coated microbeads with bioluminescence in microfluidic chips. *Biomed Microdevices* 12:683–691. doi:10.1007/s10544-010-9421-6
14. Jing W, Zhao W, Liu S, Li L, Tsai C-T, Fan X, Wu W, Li J, Yang X, Sui G (2013) Microfluidic device for efficient airborne bacteria capture and enrichment. *Anal Chem* 85:5255–5262. doi:10.1021/ac400590c
15. Mohan R, Mukherjee A, Sevgen SE, Sanpitakseree C, Lee J, Schroeder CM, Kenis PJ (2013) A multiplexed microfluidic platform for rapid antibiotic susceptibility testing. *Biosens Bioelectron* 49:118–125. doi:10.1016/j.bios.2013.04.046
16. Sun P, Liu Y, Sha J, Zhang Z, Tu Q, Chen P, Wang J (2011) High-throughput microfluidic system for long-term bacterial colony monitoring and antibiotic testing in zero-flow environments. *Biosens Bioelectron* 26:1993–1999. doi:10.1016/j.bios.2010.08.062
17. Xia N, Hunt TP, Mayers BT, Alsberg E, Whitesides GM, Westervelt RM, Ingber DE (2006) Combined microfluidic–micromagnetic separation of living cells in continuous flow. *Biomed Microdevices* 8:299–308. doi:10.1007/s10544-006-0033-0
18. Yang L, Banada PP, Chatni MR, Lim KS, Bhunia AK, Ladisch M, Bashir R (2006) A multifunctional micro-fluidic system for dielectrophoretic concentration coupled with immuno-capture of low numbers of *Listeria monocytogenes*. *Lab Chip* 6:896–905. doi:10.1039/B607061M